0022-3565/93/2673-1126$03.00/0
THE JOURNAL OF PHARMACOLOGY AND EXPERIMENTAL THERAPEUTICS
Vol. 267, No. 3
Printed in U.S.A.




# Binding and Functional Characterization of *Alpha*-2 Adrenergic Receptor Subtypes on Pig Vascular Endothelium[1]

CHARLES S BOCKMAN, WILLIAM B. JEFFRIES and PETER W. ABEL
*Department of Pharmacology, Creighton University School of Medicine, Omaha, Nebraska*
Accepted for publication August 2, 1993

**ABSTRACT**

*Alpha*-2 adrenergic receptor subtypes were characterized in membranes of pig vascular endothelium using [$^3$H]rauwolscine. *Alpha*-2 adrenergic receptor subtypes that mediate endothelium-dependent vascular relaxation were studied *in vitro* by using ring segments of pig epicardial coronary arteries. Specific [$^3$H]rauwolscine binding in endothelial membranes was saturable and to a single class of high-affinity sites with a mean $K_D$ of 0.217 ± 0.05 nM and $B_{max}$ of 156 ± 28 fmol/mg of protein. Nonlinear regression analysis indicated that competition binding curves for drugs that distinguish the *alpha*-2A adrenergic receptor subtype from the *alpha*-2C adrenergic receptor subtype fit best to two-site binding models. $K_i$ values for drugs in binding to endothelial *alpha*-2 adrenergic receptors correlated well with their $K_i$ values for *alpha*-2A ($r$ = .98) and *alpha*-2C ($r$ = .97) adrenergic receptor subtypes identified in other tissues. Vascular endothelium contained 23% *alpha*-2A and 77% *alpha*-2C adrenergic receptors. In the presence of indomethacin, the rank order of potency for agonists that cause endothelium-dependent vascular relaxation was *p*-iodoclonidine > clonidine > UK-14,304 > guanabenz > epinephrine > norepinephrine. $K_B$ values for antagonist inhibition of epinephrine-induced, endothelium-dependent vascular relaxation correlated best with $K_i$ values for antagonist binding at the *alpha*-2A adrenergic receptor subtype. These results suggest that the *alpha*-2A and *alpha*-2C adrenergic receptor subtypes are present on pig vascular endothelium and that the *alpha*-2A adrenergic receptor subtype mediates indomethacin-insensitive, endothelium-dependent relaxation of pig epicardial coronary arteries.

It is now known that there are four *alpha*-2 ADR subtypes that can be distinguished from one another based on affinity values for subtype-selective *alpha*-2 ADR antagonists. For example, the rank order of potency of subtype-selective drugs for inhibiting specific [$^3$H]rauwolscine binding to three of the *alpha*-2 ADR subtypes is oxymetazoline > BAM-1303 (8β[(2-phenylimidazol-1-yl)methyl]-6-methylergoline) > spiroxatrine > ARC-239 {2-[2,4-(O-methoxyphenyl)-piperazin-1-yl]ethyl-4,4dimethyl-1,3-(2H4H)-isoquinolindione-HCl} for the *alpha*-2A ADR, spiroxatrine > ARC-239 > BAM-1303 > oxymetazoline for the *alpha*-2B ADR and BAM-1303 > spiroxatrine > ARC-239 > oxymetazoline for the *alpha*-2C ADR (Blaxall *et al.*, 1991). In addition, it is now known that the *alpha*-2D ADR is a species homologue similar to the *alpha*-2A ADR (Bylund *et al.*, 1992). Because no single drug differentiates the *alpha*-2A ADR subtype from the *alpha*-2B ADR subtype from the *alpha*-2C ADR subtype from the *alpha*-2D ADR subtype, it is necessary to use a combination of drugs to obtain pharmacological profiles characteristic of an individual *alpha*-2 ADR subtype. Three of the four *alpha*-2 ADR subtypes have been cloned from the human genome and the binding characteristics of the expressed receptors confirm the pharmacological classification of *alpha*-2A, *alpha*-2B and *alpha*-2C ADR subtypes (Bylund *et al.*, 1992).

Functional studies suggest the presence of *alpha*-2 ADRs on vascular endothelium. For example, in isolated coronary arteries, norepinephrine and clonidine cause endothelium-dependent relaxation that is inhibited by selective *alpha*-2 ADR antagonists such as rauwolscine (Cocks and Angus, 1983; Vanhoutte and Miller, 1989). Similar results were found using several different isolated arteries (Angus *et al.*, 1986) and veins (Miller and Vanhoutte, 1985). It has also been reported that endothelium-dependent, *alpha*-2 ADR-induced relaxation of pig coronary arteries is mediated by an endothelium-derived relaxing factor, nitric oxide (Richard *et al.*, 1990). We recently reported that norepinephrine-induced release of an endothelium-derived relaxing factor, nitric oxide, is enhanced in mineralocorticoid hypertension (Bockman *et al.*, 1992). Taken together, these results suggest that endothelial *alpha*-2 ADRs may play an important role in regulating vascular tone in both normal and pathological conditions.

The *alpha*-2 ADR subtypes present on vascular endothelium

Received for publication February 12, 1993.
[1] This work was supported by the American Heart Association- Nebraska Affiliate.

**ABBREVIATIONS:** ADR, adrenergic receptor; $K_B$, functional equilibrium dissociation constant; $K_i$, inhibition binding equilibrium dissociation constant; $K_{iH}$, high-affinity inhibition binding equilibrium dissociation constant; $K_{iL}$, low-affinity inhibition binding equilibrium dissociation constant.

are unknown. Thus, we characterized the *alpha*-2 ADR subtypes present on pig vascular endothelium by determining the affinities of several *alpha*-2 ADR subtype-selective drugs for inhibiting specific [$^3$H]rauwolscine binding. We also determined the affinities of *alpha*-2 ADR subtype-selective drugs in inhibiting endothelium-dependent, *alpha*-2 ADR-mediated relaxation of pig coronary arteries. Furthermore, we correlated the binding affinities with the affinities obtained from functional studies to determine which *alpha*-2 ADR subtype mediates endothelium-dependent vascular relaxation.

## Methods

**Drugs.** The drugs used were obtained from the following sources: oxymetazoline HCl, indomethacin, (−)-epinephrine bitartrate, (−)-norepinephrine bitartrate, clonidine HCl, nadolol, desipramine HCl and guanabenz (Sigma, St. Louis, MO); rauwolscine HCl, spiroxatrine, *p*-iodoclonidine HCl, prazosin HCl and phentolamine mesylate (Research Biochemicals, Natick, MA); UK 14,304 (5-bromo-6-[2-imidazoline-2-yl-amino]quinoxaline) (Pfizer Central Research, Sandwich, England); ARC-239 (Thomae, Biberach, Germany); SKF 104856 (2-vinyl-7-chloro-3,4,5,6-tetrahydro-4-methyl-thieno[4,3,2ef][3]benzazepine) (SmithKline Beecham Pharmaceuticals, King of Prussia, PA); BAM-1303 (kindly provided by Dr. David Bylund, Department of Pharmacology, University of Nebraska Medical Center, Omaha, NE); and [$^3$H] rauwolscine (78 Ci/mmol; New England Nuclear, Boston, MA).

**Endothelial membrane preparation.** Pig thoracic aortas were obtained from a local slaughterhouse, cleaned of fat and connective tissue and placed into ice-cold Krebs' solution (in millimolar composition: NaCl, 120; KCl, 5.5; $CaCl_2$, 2.5; $NaH_2PO_4$, 1.4; $MgCl_2$, 1.2; $NaHCO_3$, 20; dextrose, 11.1; $CaNa_2$-EDTA, 0.027) equilibrated with 95% $O_2$/5% $CO_2$ for transport to the laboratory. The aortas were cut longitudinally and pinned down on Styrofoam backing. The luminal surface was washed with ice-cold isotonic phosphate-buffered saline containing 137 mM NaCl, 2.7 mM KCl, 8.1 mM $Na_2HPO_4$ and 1.5 mM $KH_2PO_4$, pH 7.6. Luminal scrapings of vascular endothelium were obtained by passing a number 10 scalpel blade, held at a 45° angle, over the luminal surface of the aorta. The scrapings were pooled in 10 ml of ice-cold phosphate-buffered saline for washing by centrifugation at 3000 × *g* at 4°C for 15 min. The pellet was resuspended in 10 ml of 50 mM Tris HCl, pH 8.0, and homogenized with a Tekmar Tissuemizer (Cincinnati, OH) at a setting of 80 for 20 sec. The homogenate was centrifuged at 35,000 × *g* at 4°C for 20 min. The pellet was stored at −80°C.

**Radioligand binding assays.** The pellet was resuspended and homogenized in 200 volumes of 25 mM glycylglycine buffer, pH 7.6. For saturation binding experiments, total [$^3$H]rauwolscine binding was determined using duplicate tubes containing 970 μl of membrane suspension, 10 μl of 5 mM HCl and 20 μl of [$^3$H]rauwolscine, which ranged in concentration from 0.02 to 2 nM. To a parallel set of duplicate tubes, 10 μl of 100 μM (−)-norepinephrine in 5 mM HCl were added to determine nonspecific binding. After a 45-min incubation in a shaking water bath at 25°C, membrane suspensions were filtered through GF/B glass fiber filter strips (Whatman, Clifton, NJ) using a 48-sample cell harvester (Brandel, Gaithersburg, MD). Tubes and filters were washed four times with 5 ml of ice-cold 50 mM Tris HCl (pH 8.0) and radioactivity retained on the filters counted by liquid scintillation spectroscopy. Specific binding was calculated as the difference between total and nonspecific binding. For competition binding experiments, duplicate tubes containing 970 μl of membrane suspension, 20 μl of [$^3$H]rauwolscine (0.1 nM final concentration) and 10 μl of increasing concentrations of various unlabeled drugs were incubated and processed as for saturation experiments. The protein concentration was determined by the method of Lowry *et al.* (1951) by using bovine serum albumin as the standard.

The binding data were analyzed using a nonlinear least-squares curve-fitting program to determine $K_D$ and $B_{max}$ values from saturation binding experiments and $IC_{50}$ values from competition binding experiments. $K_I$ values were calculated from $IC_{50}$ values by using the method of Cheng and Prusoff (1973). All values are given as means ± S.E. The *F* test was used to determine whether or not the binding data fit best to a one- or two-site binding model. A value of $P < .05$ was used to conclude that the two-site model fit the data best.

**Measurements of endothelium-dependent relaxation of coronary arteries.** The proximal third of the left circumflex coronary arteries was dissected from pig hearts obtained from a local slaughterhouse. The arteries were cleaned of fat and adhering tissue, cut into 3-mm long ring segments and mounted between two stainless steel pins passed through the lumen of the rings. Ring segments were placed in water-jacketed glass muscle chambers that contained Krebs' solution maintained at 37°C gassed with 95% $O_2$/5% $CO_2$, pH 7.4. One pin was attached to a Grass FT.03 force transducer for measurement of isometric tension with a Grass polygraph (Quincy, MA). After a 1-hr equilibration period at 6 g of resting tension (determined to be optimum in preliminary length-tension experiments), ring segments were contracted with a maximal contractile concentration (45 mM) of KCl and then washed for 30 min. Ring segments were then contracted to one-half of maximal contraction with KCl and, when the response reached a stable level of tone, cumulative concentration-response relaxation curves for agonists were generated. Relaxation-response curves were obtained in the presence of 10 μM indomethacin to inhibit production of cyclooxygenase products, 0.1 μM desipramine to inhibit neuronal uptake of catecholamines, 0.1 μM prazosin to block *alpha*-1 ADR-mediated contraction and 10 μM nadolol to block *beta* ADR-mediated relaxation. To quantify potency values of agonists, the $EC_{50}$ for the relaxation responses was calculated from concentration-response curves by linear regression of all points between 20% and 80% of the maximal response. $EC_{50}$ values are expressed as means ± S.E.

**Functional determination of antagonist affinity values.** The $pA_2$ value for the selective *alpha*-2 ADR antagonist rauwolscine was calculated as described by Arunlakshana and Schild (1959). After the determination of control concentration-response curves for epinephrine, the tissues were washed and equilibrated for 1 hr with 10 nM rauwolscine. Then epinephrine concentration-response curves were repeated. The tissues were then thoroughly washed with Krebs' solution and equilibrated for 1 hr with 30 nM rauwolscine before repeating the epinephrine concentration-response curves. This same sequence was repeated again using 100 nM rauwolscine. Dose ratios of $EC_{50}$ values in the presence and absence of rauwolscine were calculated and Schild plots were constructed by plotting the log of the dose ratio minus 1 *versus* the log of the concentration of rauwolscine. Linear regression of the plotted points was used to determine the *x*-intercept ($pA_2$). The slopes of the Schild regressions were considered different from unity if the 95% confidence interval did not include the value of 1. The $pA_2$ values were converted to their antilogs and expressed as $K_B$ values. The $K_B$ values for the *alpha* adrenergic antagonists, ARC-239, prazosin, SKF-104856 and spiroxatrine, were calculated as described by Mackay (1978). After the determination of control concentration-response curves for epinephrine, the tissues were washed and equilibrated for 1 hr with a single concentration of antagonist and epinephrine concentration-response curves were repeated. Antagonist concentrations, predicted to cause 10-fold shifts in concentration-response curves, were chosen based on the data from preliminary experiments. The $K_B$ values were determined from the following equation: $\log K_B = \log [\text{antagonist}] - \log (\text{dose ratio} - 1)$, where the dose ratio = $EC_{50}$ in the presence of antagonist divided by $EC_{50}$ in the absence of antagonist. Time control experiments were performed and showed that concentration-response curves for epinephrine did not change over the time required to conduct antagonist affinity determinations.

## Results

**Radioligand binding experiments.** [$^3$H]Rauwolscine binding in vascular endothelial membranes is shown in figure 1A. Nonlinear regression analysis of individual saturation binding isotherms indicated that [$^3$H]rauwolscine bound with high

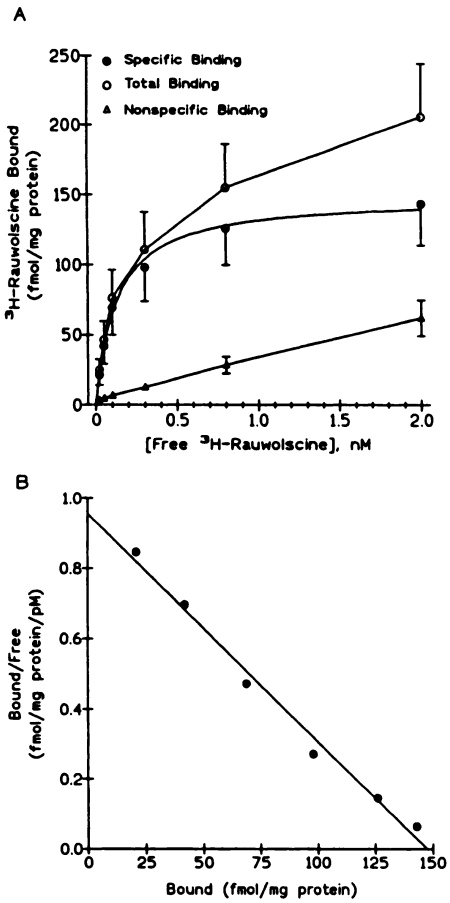


**Fig. 1.** A) Illustrates mean saturation binding isotherms for [$^3$H]rauwolscine in pig vascular endothelial membranes. Concentrations of free [$^3$H]rauwolscine, ranging from 0.02 to 2.0 nM, were incubated with endothelial membranes (0.150 mg/ml of assay volume) in the presence (nonspecific binding) and absence (total binding) of 100 $\mu$M (−)-norepinephrine. Nonlinear regression analysis of six individual specific binding isotherms indicated that [$^3$H]rauwolscine bound to a homogeneous population of binding sites with a mean $K_D$ value of 0.217 ± 0.05 nM and $B_{max}$ of 156 ± 28 fmol/mg of protein. Specific [$^3$H]rauwolscine binding was 70% to 90% of total binding. B) Shows a mean Rosenthal plot derived from six individual experiments.

affinity to a single class of binding sites. The mean $K_D$ value for [$^3$H]rauwolscine in binding to *alpha*-2 ADRs on endothelial membranes was 0.217 ± 0.05 nM and the $B_{max}$ was 156 ± 28 fmol/mg of protein. Specific [$^3$H]rauwolscine binding was 90% of total binding at the $K_D$ concentration. Figure 1B illustrates a mean Rosenthal plot derived from individual saturation binding isotherms.

The $K_I$ for rauwolscine inhibition of specific [$^3$H]rauwolscine binding in endothelial membranes was determined from competition binding studies (fig. 2). Individual competition binding curves for rauwolscine fit best to a one-site binding model; this was consistent with the results from saturation binding experiments. The mean $K_I$ value (0.261 ± 0.07 nM) for rauwolscine agreed well with the $K_D$ value for [$^3$H]rauwolscine from saturation binding experiments. $K_D$ and $K_I$ values for rauwolscine were consistent with binding to *alpha*-2 ADRs. In addition, the rank order of potency (rauwolscine > ARC-239 > prazosin) for inhibiting specific [$^3$H]rauwolscine binding in endothelial membranes was consistent with [$^3$H]rauwolscine binding to *alpha*-2 ADRs (table 1).

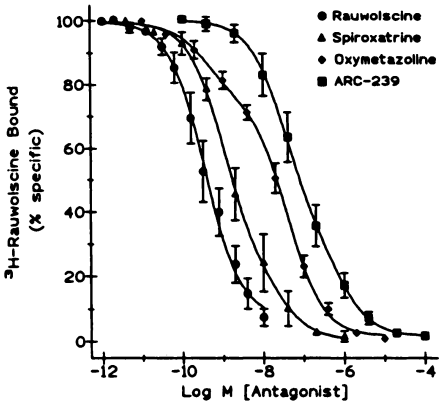


**Fig. 2.** Mean competition binding curves showing *alpha*-2 adrenergic antagonists inhibition of specific [$^3$H]rauwolscine binding. For each concentration of antagonist, [$^3$H]rauwolscine binding is expressed as a percentage of the specific binding in the absence of any drug. One- and two-site binding models were fit to individual competition binding curves by using a nonlinear least-squares curve-fitting program to obtain $K_I$ values. Competition binding curves for rauwolscine fit best to a one-site binding model; competition binding curves for spiroxatrine, oxymetazoline and ARC-239 fit best to a two-site binding model.

We determined $K_I$ values (table 1) for SKF-104856 and BAM-1303 in inhibiting specific [$^3$H]rauwolscine binding in endothelial membranes to determine whether or not the *alpha*-2B ADR subtype was present. SKF-104856 differentiates the *alpha*-2B ADR subtype ($K_I$ < 10 nM) from the *alpha*-2A and *alpha*-2C ADR subtypes ($K_I$s = 50–200 nM; Gleason and Hieble, 1991; Simonneaux *et al.*, 1991). However, SKF-104856 does not differentiate the *alpha*-2A ADR subtype from the *alpha*-2C ADR subtype. The $K_I$ value for SKF-104856 in binding to *alpha*-2 ADRs on endothelial membranes was 54.5 nM, consistent with binding to either the *alpha*-2A ADR, *alpha*-2C ADR or both receptor subtypes. Similar to SKF-104856, BAM-1303 also identifies the *alpha*-2B ADR subtype ($K_I$ = 7–26 nM) from the *alpha*-2A and *alpha*-2C ADR subtypes ($K_I$s = 0.4–2.5 nM; Blaxall *et al.*, 1991; Bylund *et al.*, 1992). The $K_I$ value for BAM-1303 in binding to *alpha*-2 ADRs on endothelial membranes was 0.394 nM. These results suggest the presence of the *alpha*-2A or *alpha*-2C ADR subtypes, or both, on endothelial membranes. $K_I$ values for SKF-104856 and BAM-1303 also suggest that the *alpha*-2B ADR subtype is not present on pig vascular endothelium.

$K_I$ values for rauwolscine and BAM-1303 in inhibiting specific [$^3$H]rauwolscine binding in endothelial membranes were obtained to determine whether or not the *alpha*-2D ADR subtype was present. Because rauwolscine and BAM-1303 have relatively low affinities ($K_I$ = 3.4 nM and 53 nM, respectively; Simonneaux *et al.*, 1991) for the *alpha*-2D ADR subtype compared with the *alpha*-2A, *alpha*-2B and *alpha*-2C ADR subtypes, both drugs can distinguish the *alpha*-2D ADR subtype from the other three *alpha*-2 ADR subtypes. Our high-affinity $K_I$ values for rauwolscine (0.261 nM) and BAM-1303 (0.394 nM) in inhibiting specific [$^3$H]rauwolscine binding in endothelial membranes indicate that the *alpha*-2D ADR subtype is not present on pig vascular endothelial membranes.

We also determined $K_I$ values (table 1) from competition binding experiments (fig. 2) for ARC-239, spiroxatrine and

TABLE 1

**Affinities of *alpha*-2 ADR antagonists for inhibiting specific [$^3$H]rauwolscine binding ($K_I$) in vascular endothelium and for inhibiting endothelium-dependent vascular relaxation ($K_B$)**

The values are means ± S.E.; $n$ = number of endothelial cell preparations or arteries from individual animals. Binding data were analyzed using a nonlinear least-squares curve-fitting computer program. Affinity values from binding data that fit best to a two-site binding model are expressed as $K_H$ (high-affinity binding site) and $K_L$ (low-affinity binding site). %High = percent of high-affinity binding sites; %Low = percent of low-affinity binding sites.

| Drug | $K_I$ | $K_H$ | %High | $K_L$ | %Low | $K_B$ |
|---|---|---|---|---|---|---|
| | nM | nM | | nM | | nM |
| Rauwolscine | 0.261 ± 0.07 ($n$ = 5) | | | | | 1.71 ± 0.26 ($n$ = 4) |
| SKF-104856 | 54.5 ± 10.0 ($n$ = 2) | | | | | 42.7 ± 4.6 ($n$ = 3) |
| BAM-1303 | 0.394 ± 0.14 ($n$ = 2) | | | | | ND[a] |
| ARC-239 | | 26.4 ± 8.4 ($n$ = 6) | 72 | 544 ± 180 ($n$ = 6) | 28 | 1290 ± 140 ($n$ = 6) |
| Prazosin | | 51.4 ± 5.3 ($n$ = 2) | 86 | 1620 ± 390 ($n$ = 2) | 14 | 1480 ± 170 ($n$ = 4) |
| Spiroxatrine | | 0.595 ± 0.08 ($n$ = 3) | 77 | 17.8 ± 4.0 ($n$ = 3) | 23 | 24.6 ± 3.8 ($n$ = 6) |
| Oxymetazoline | | 0.258 ± 0.11 ($n$ = 5) | 26 | 27.0 ± 6.2 ($n$ = 5) | 74 | ND[a] |

[a] Not determined.

oxymetazoline in inhibiting specific [$^3$H]rauwolscine binding to determine whether or not the *alpha*-2A ADR, *alpha*-2C ADR or both receptor subtypes were present on endothelial membranes. ARC-239 distinguishes the *alpha*-2A ADR subtype ($K_I$ = 171 nM) from the *alpha*-2B and *alpha*-2C ADR subtypes ($K_I$s = 2–13 nM; Bylund *et al.*, 1992). In our experiments, ARC-239 bound to a heterogeneous population of *alpha*-2 ADRs on endothelial membranes with a $K_{IH}$ value of 26.4 nM and a $K_{IL}$ value of 544 nM, consistent with binding to *alpha*-2A and *alpha*-2C ADR subtypes. We also obtained similar results using prazosin (table 1). Like ARC-239, spiroxatrine also distinguishes the *alpha*-2A ADR subtype ($K_I$ = 8–13 nM) from the *alpha*-2B and *alpha*-2C ADR subtypes ($K_I$s = 0.3–0.6 nM; Blaxall *et al.*, 1991; Bylund *et al.*, 1992). In our study, spiroxatrine also bound to a heterogeneous population of *alpha*-2 ADRs on endothelial membranes with a $K_{IH}$ value of 0.595 nM and a $K_{IL}$ value of 17.8 nM, consistent with binding to *alpha*-2A and *alpha*-2C ADR subtypes. Oxymetazoline also differentiates the *alpha*-2A ADR subtype ($K_I$ = 0.8–1.5 nM) from the *alpha*-2B and *alpha*-2C ADR subtypes ($K_I$s = 31–300 nM; Blaxall *et al.*, 1991; Bylund *et al.*, 1992). In endothelial membranes, oxymetazoline bound to two pharmacologically distinct *alpha*-2 ADR sites with $K_{IH}$ and $K_{IL}$ values of 0.258 nM and 27.0 nM, respectively. Using these antagonists, we found from 14% to 28% *alpha*-2A ADRs and from 72% to 86% *alpha*-2C ADRs (table 1). Taken together, these results suggest that pig vascular endothelium contains both *alpha*-2A and *alpha*-2C ADR subtypes.

**Functional measurements of antagonist affinity.** Mean concentration-response curves for *alpha*-2 ADR agonists in causing relaxation of pig left circumflex coronary arteries are shown in figure 3. The rank order of potency was *p*-iodoclonidine > clonidine > UK 14,304 > guanabenz > epinephrine > norepinephrine, which suggests *alpha*-2 ADRs mediate relaxation of pig coronary arteries. Compared with epinephrine, UK 14,304 and norepinephrine were full agonists, whereas *p*-iodoclonidine, clonidine and guanabenz were partial agonists. In arteries without endothelium, epinephrine did not cause relaxation, which suggests *beta* adrenergic receptors were effectively blocked in our experiments. These results suggest *alpha*-2 ADRs located on the endothelium mediate relaxation of pig coronary arteries.

To determine the affinity of rauwolscine for inhibiting endothelium-dependent, *alpha*-2 ADR-mediated relaxation in coronary arteries, we generated epinephrine concentration-response curves in the presence of increasing concentrations of rauwolscine (fig. 4A). Rauwolscine-induced shifts in the epinephrine concentration-response curves are plotted according to the method of Arunlakshana and Schild (1959, fig. 4B). Slopes of individual Schild regressions from four separate experiments were not different from unity; therefore, the slopes of regression lines were constrained to one for determining $pA_2$ values (slope of Schild regressions = −1.20 ± 0.03; $pA_2$ value for rauwolscine = 1.71 ± 0.26 nM). Table 1 lists affinity values for rauwolscine, ARC-239, prazosin, SKF-104856 and spiroxatrine in inhibiting endothelium-dependent, *alpha*-2 ADR-mediated vascular relaxation.

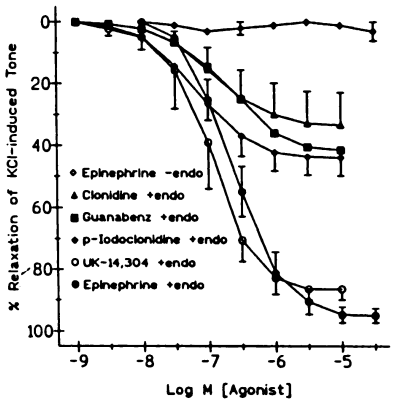


**Fig. 3.** Mean concentration-response curves for *alpha*-2 adrenergic agonists in causing relaxation of pig left circumflex coronary arteries with (+endo) and without (−endo) endothelium in the presence of nadolol (10 μM), prazosin (0.1 μM), desipramine (0.1 μM) and indomethacin (10 μM). Relaxation responses are expressed as the percent relaxation to the base-line level of the tone present before KCl addition. $EC_{50}$ values for agonists in nanomolar concentration are: epinephrine, 240 ± 62; UK 14,304, 147 ± 50; *p*-iodoclonidine, 64.6 ± 22; guanabenz, 170 ± 60; clonidine, 144 ± 40; and norepinephrine, 1100 ± 280 (data not shown). Each curve represents mean responses of three to five arteries taken from individual animals.

**Correlation of binding with function.** Table 1 lists antagonist affinity values for *alpha*-2A and *alpha*-2C ADR binding sites ($K_I$s) on vascular endothelium and for inhibiting endothelium-dependent, *alpha*-2 ADR-mediated vascular relaxation ($K_B$s). $K_B$ values were similar to $K_I$ values at the *alpha*-2A ADR subtype. By contrast, $K_B$ values for subtype-selective drugs were 30- to 50-fold different compared with $K_I$ values at the *alpha*-2C ADR subtype. Figure 5 illustrates this comparison between $K_B$ and $K_I$ values. The $K_B$ *versus* $K_I$ comparison at the *alpha*-2A ADR subtype correlated well ($r$ = .98). In most cases,

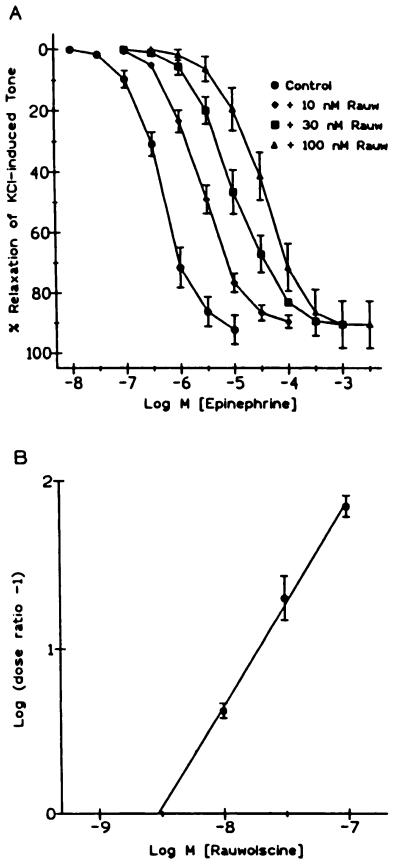


**Fig. 4.** A) Illustrates mean concentration-response curves for epinephrine-induced relaxation of pig left circumflex coronary arteries with endothelium in the absence (Control) and presence (+Rauw) of rauwolscine. Relaxation response curves are plotted as the percent relaxation to the base-line level of tone present before KCl addition. B) Shows a mean Schild plot of four individual experiments. Rauwolscine-induced shifts in the epinephrine relaxation-response curves are expressed as the log of the dose ratio − 1.

the 95% confidence intervals of the plotted points contained the line of identity, which illustrates the similarity between $K_B$ and $K_I$ values at the *alpha*-2A ADR subtype. Conversely, the regression line correlating antagonist $K_I$s for the *alpha*-2C ADR subtype with $K_B$s was significantly different from the line of identity and the comparison did not correlate as well ($r = .80$). Taken together, these data suggest that the *alpha*-2A ADR subtype mediates endothelium-dependent relaxation of pig coronary arteries.

## Discussion

The existence of a heterogeneous population of *alpha*-2 ADRs is now well established. Radioligand binding and molecular cloning studies both indicate the presence of four subtypes of *alpha*-2 ADRs (Bylund, 1992; Harrison *et al.*, 1991). The pharmacological characterization of these receptor subtypes is based on radioligand binding studies in tissues and cell lines containing only one subtype. Using the human colonic adenocarcinoma cell line (HT29 cell; *alpha*-2A), neonatal rat lung (*alpha*-2B), the opossum kidney cell line (OK cell; *alpha*-2C) (Blaxall *et al.*, 1991) and the bovine pineal gland (*alpha*-2D) (Simonneaux *et al.*, 1991), Bylund and coworkers identified drugs with different binding affinities for the four *alpha*-2 ADR subtypes. *Alpha*-2 ADR subtypes can be distinguished from one another based on these differential affinity values for subtype-selective *alpha*-2 ADR antagonists. Using several subtype-selective *alpha*-2 ADR drugs, we characterized the *alpha*-2 ADR subtypes present on vascular endothelium. We also studied the functional role of *alpha*-2 ADR subtypes in mediating endothelium-dependent vascular relaxation.

Using drugs that distinguish the *alpha*-2B and *alpha*-2D ADR subtypes from the *alpha*-2A and *alpha*-2C ADR subtypes, we determined that the *alpha*-2B and *alpha*-2D ADR subtypes are not present on pig vascular endothelial membranes. For example, in vascular endothelial membranes, $K_I$ values for BAM-1303 and SKF-104856 were 10- to 50-fold different from their $K_I$s at the *alpha*-2B ADR subtype (Blaxall *et al.*, 1991; Bylund *et al.*, 1992; Gleason and Hieble, 1991). In vascular endothelial membranes, $K_I$ values for BAM-1303 and rauwolscine were different by 135-fold and 13-fold, respectively, from their $K_I$s at the *alpha*-2D ADR subtype (Simonneaux *et al.*, 1991). However, the $K_I$ values for rauwolscine, BAM-1303 and SKF-104856 in endothelial membranes are consistent with their $K_I$s at the *alpha*-2A and *alpha*-2C ADR subtypes (Blaxall *et al.*, 1991; Bylund *et al.*, 1992; Gleason and Hieble, 1991). The competition binding curves for rauwolscine, BAM-1303 and SKF-104856 in endothelial membranes fit best to one-site binding models, which was consistent with their lack of selectivity between the *alpha*-2A and *alpha*-2C ADR subtypes.

We identified a heterogeneous population of *alpha*-2 ADR

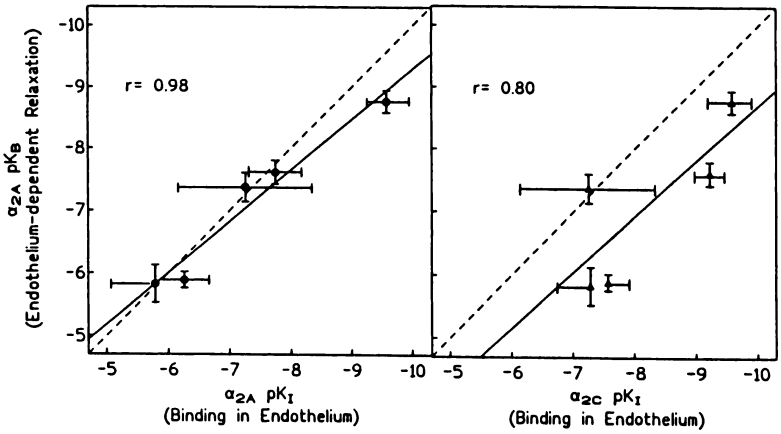


**Fig. 5.** Correlation plots of affinity values for ARC-239, prazosin, spiroxatrine, SKF-104856 and rauwolscine for inhibiting *alpha*-2 ADR-mediated, endothelium-dependent relaxation ($pK_B$, *y*-axis) and for inhibiting specific [$^3$H]rauwolscine binding in endothelial membranes ($pK_I$, *x*-axis). Affinity values are expressed as the mean ± 95% confidence interval and are taken from table 1. The dashed line represents the line of identity and the solid line, the regression line of the plotted points. The correlation coefficient (*r*) is listed.

DOCKET ALARM

# Explore Litigation Insights

Docket Alarm provides insights to develop a more informed litigation strategy and the peace of mind of knowing you're on top of things.

## Real-Time Litigation Alerts

Keep your litigation team up-to-date with **real-time alerts** and advanced team management tools built for the enterprise, all while greatly reducing PACER spend.

Our comprehensive service means we can handle Federal, State, and Administrative courts across the country.

## Advanced Docket Research

With over 230 million records, Docket Alarm's cloud-native docket research platform finds what other services can't. Coverage includes Federal, State, plus PTAB, TTAB, ITC and NLRB decisions, all in one place.

Identify arguments that have been successful in the past with full text, pinpoint searching. Link to case law cited within any court document via Fastcase.

## Analytics At Your Fingertips

Learn what happened the last time a particular judge, opposing counsel or company faced cases similar to yours.

Advanced out-of-the-box PTAB and TTAB analytics are always at your fingertips.

## API

Docket Alarm offers a powerful API (application programming interface) to developers that want to integrate case filings into their apps.

**LAW FIRMS**
Build custom dashboards for your attorneys and clients with live data direct from the court.

Automate many repetitive legal tasks like conflict checks, document management, and marketing.

**FINANCIAL INSTITUTIONS**
Litigation and bankruptcy checks for companies and debtors.

**E-DISCOVERY AND LEGAL VENDORS**
Sync your system to PACER to automate legal marketing.